Scanning Microscopy

Volume 1995
Number 9 *Luminescence*

Article 22

1995

Temperature-Dependent Cathodoluminescence Spectroscopy and Microscopy as a Tool for Defect Identification in Semiconducting Ceramics: Application to BaTiO3 Ceramics

T. Hübner
Martin-Luther-Universität Halle, Germany

U. Marx
Martin-Luther-Universität Halle, Germany

J. Schreiber
Martin-Luther-Universität Halle, Germany

Scanning Microscopy Supplement 9, 1995 (Pages 263-268) 0892-953X/95$5.00+.25
Scanning Microscopy International, Chicago (AMF O'Hare), IL 60666 USA

TEMPERATURE-DEPENDENT CATHODOLUMINESCENCE SPECTROSCOPY AND MICROSCOPY AS A TOOL FOR DEFECT IDENTIFICATION IN SEMICONDUCTING CERAMICS: APPLICATION TO $BaTiO_3$ CERAMICS

T. Hübner*, U. Marx[1] and J. Schreiber

Martin-Luther-Universität Halle, Fachbereich Physik,
Friedemann-Bach-Platz 6, D-06108 Halle, Germany

Abstract

Cathodoluminescence (CL) spectroscopy and microscopy were applied to investigate the characteristic grain-boundary contrast in semiconducting ferroelectric $BaTiO_3$ ceramics. It was shown, that "chemically clean" grain boundaries do not reveal any specific CL components neither in the visible nor in the infrared part of the spectrum. Instead, the contrast arises from at least two different non-radiative recombination centers present in the grain and the grain-boundary zones, respectively. Activation thresholds for these centers were determined from the temperature dependence of the integral CL signal down to 30K. The different values found explain the contrast reversal observed in $BaTiO_3$ ceramics upon cooling. Starting from a consideration of the defect equilibria present in the samples after selected treatment cycles, we could attribute the non-radiative recombination centers to oxygen vacancies.

Key Words: $BaTiO_3$ ceramics, PTC effect, cathodoluminescence spectroscopy, cathodoluminescence microscopy, grain-boundary contrast, barium vacancies, oxygen vacancies, radiative recombination, non-radiative recombination, activation energy.

[1]Deceased, December 12, 1995.

*Address for correspondence and present address:
Torsten Hübner
Mannheimer Straβe 60,
D-04209 Leipzig
Germany

Telephone number: 49-341 4215 727
FAX number: 49-341 4975 403

Introduction

The well-known cathodoluminescence (CL) grain-boundary contrast observed in PTC (positive temperature coefficient) $BaTiO_3$ ceramics has been studied to some extent by Koschek and Kubalek (1983, 1985). At room temperature, in integral CL micrographs from PTC $BaTiO_3$ ceramics, the grain boundaries appear dark. In Y-doped samples, Koschek and Kubalek (1983, 1985) found the reverse contrast (light grain boundaries) within the near infrared (IR) spectral range. Koschek and Kubalek (1983, 1985) attributed the energy of the IR recombination signal from grain boundaries to a transition including the doubly ionized Ba vacancy level in the $BaTiO_3$ band structure model (Daniels and Wernicke, 1976). CL experiments on La-doped $BaTiO_3$ ceramics by the present authors (Hübner *et al.*, 1993), however, could not confirm that Ba vacancies at grain boundaries act as radiative recombination centers in the IR, thereby quenching the CL signal in the visible spectral range.

In this paper, we will be concerned with temperature-dependent CL spectroscopy and microscopy from La-doped $BaTiO_3$ ceramics aimed to an identification of the recombination centers present in that material. For this purpose, a few samples were treated in a reducing atmosphere to modify the intrinsic defect concentration, in particular, the oxygen vacancy concentration.

Experimental Procedure

The $BaTiO_3$ ceramic samples were prepared using the conventional mixed oxide technique (Abicht *et al.*, 1991). The sample composition was $Ba_{0.998}La_{0.002}TiO_3$ + 4 mol% TiO_2. After calcination, the samples were heated at a rate of 2 K/min, then sintered in air at 1400°C for 1 hour and slowly cooled down at a rate of 10 K/min. All samples showed the PTC effect. Samples designated R1 and R2 were annealed in a reducing atmosphere under the conditions summarized in Table 1. The samples were ground to remove the sintering skin and finally polished with diamond

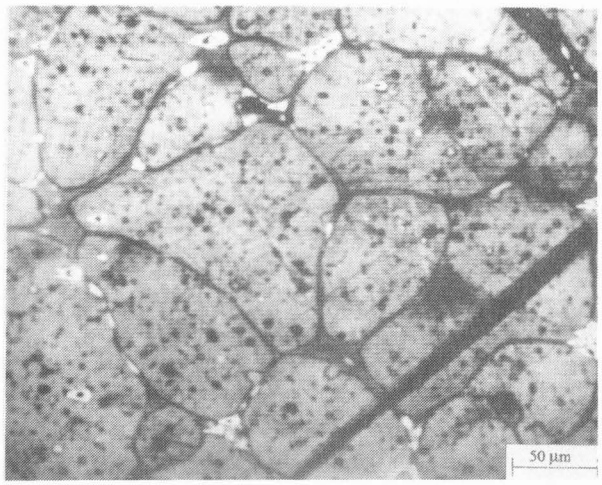

Figure 1. CL micrograph of La-doped $BaTiO_3$ ceramic at 293K in the visible spectral range.

Table 1. Parameters of the reducing treatment

	oxygen partial pressure	temperature	annealing time
R1	1 Pa	800°C	15 minutes
R2	10^{-15} Pa	1000°C	15 minutes

suspension to yield a scratch-free surface.

The samples were investigated using a scanning electron microscope equipped with CL equipment and cooling facilities. The CL micrographs were taken using a multi-alkali photomultiplier with S20 characteristic. CL spectra were recorded using a cooled GaAs or a InGaAs photomultiplier, the non-linear sensitivity of which was corrected for.

Results

A CL micrograph of the non-reduced specimen taken at 293K in the visible spectral range is shown in Figure 1. Clearly, a pronounced contrast between grains and grain boundaries is visible. The light spots in the CL micrograph are secondary phases caused by impurities like silicon. In Figure 2, CL spectra taken at 293K from grain interior and grain boundary zones are shown. Both spectra have the same broad structure with a maximum at 2.4 eV corresponding to 516 nm. Significant differences in the spectral composition do not exist. In particular, an IR signal from grain boundaries cannot be observed up to 1030 nm. The line scan across a grain boundary shown in Figure 3 further demonstrates that the CL intensity in fact is decreased at the grain

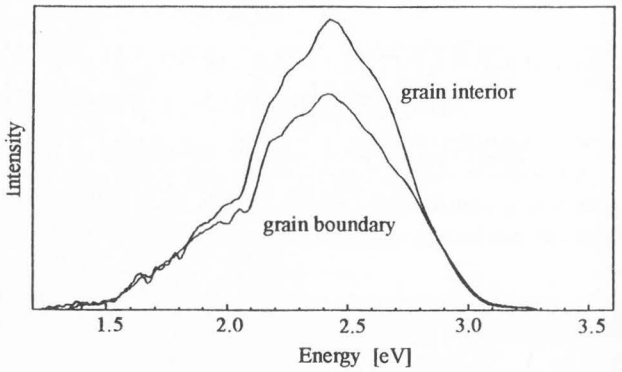

Figure 2. CL spectra from grain and grain-boundary zones at 293K.

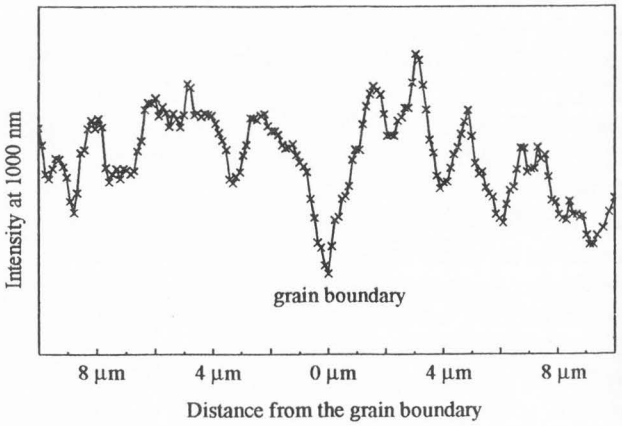

Figure 3. Line scan at 1000 nm across a grain boundary at 293K.

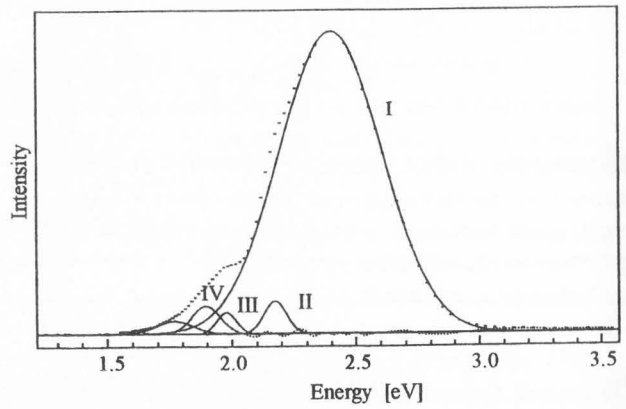

Figure 4. CL spectrum at 33K and decomposition into Gaussian components I-IV.

---

boundary in the near IR spectral range up to 1030 nm.

CL observations from $BaTiO_3$ ceramics with additional dopants like Mn and/or substitutes like Ca, additives like Si, as well as from Y-doped $BaTiO_3$ ceramics all have revealed principally the same CL spectrum from grains and grain boundaries (Hübner, 1994). This even

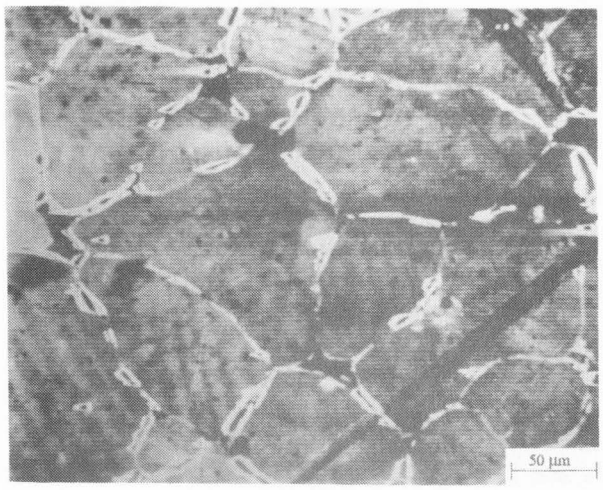

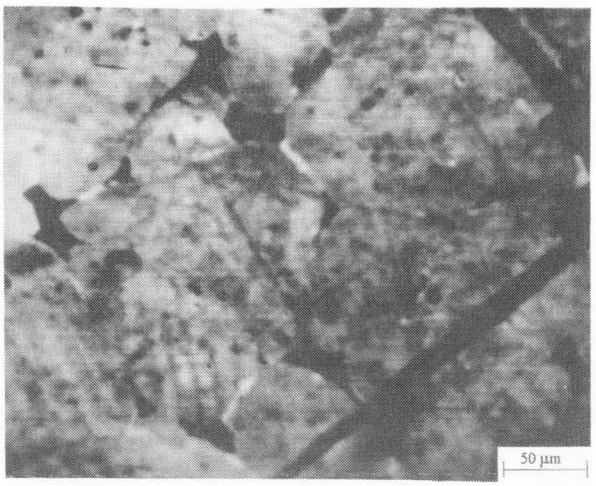

Figures 5 and 6. CL micrographs at 77K (**Fig. 5, at left**) and at 50K (**Fig. 6, at right**) in the visible spectral range.

Table 2. Gaussian decomposition of low-temperature CL spectra.

	Max. I (eV)	FWHM (eV)	Max. II (eV)	FWHM (eV)	Max. III (eV)	FWHM (eV)	Max. IV (eV)	FWHM (eV)
grain interior	2.40 (94%)	0.48	2.17 (2%)	0.11	1.98 (1%)	0.09	1.89 (3%)	0.14
grain boundary	2.37 (93%)	0.49	2.18 (1%)	0.11	1.96 (2%)	0.16	1.85 (4%)	0.27

Max. = Maxima FWHM = Full width at half maximum.

holds at temperatures as low as 30K.

In Figure 4, a CL spectrum taken at 33K is given together with its Gaussian decomposition. The parameters of the Gaussian components from grain and grain-boundary spectra are shown in Table 2. The essential part of the CL spectrum is related to a radiative recombination mechanism centered at approximately 2.4 eV. This observation is valid for the CL spectra from all $BaTiO_3$ ceramics investigated so far, no matter whether they were taken from grains or from grain boundaries (Hübner, 1994).

A CL micrograph in the visible spectral range taken at 77K is presented in Figure 5. The CL contrast now is reverse compared to Figure 1. At 50K, however, as illustrated in Figure 6, only a few grain boundaries are brighter than the grains.

The logarithm of the normalized integral CL intensity from 350 nm to 850 nm is plotted versus 1/T (T = temperature) in Figure 7. Three subsequent intervals of linear slope, different for grain interior and grain

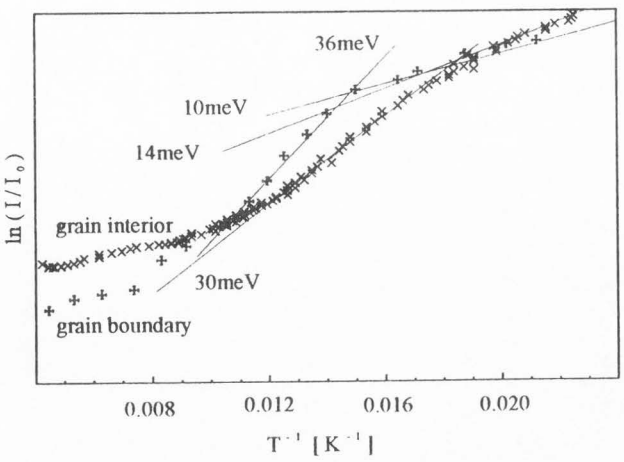

Figure 7. Logarithm of the normalized integral CL intensity in the visible spectral range against 1/T for grain and grain-boundary zones.

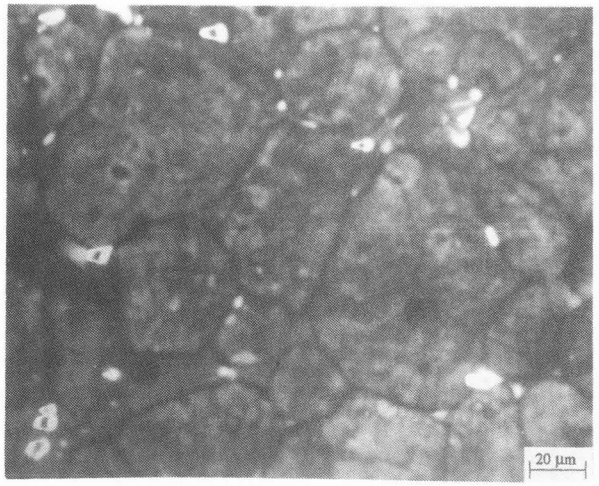

Figure 8. CL micrograph from the La-doped $BaTiO_3$ ceramic sample R1 annealed in a weakly reducing atmosphere at 293K.

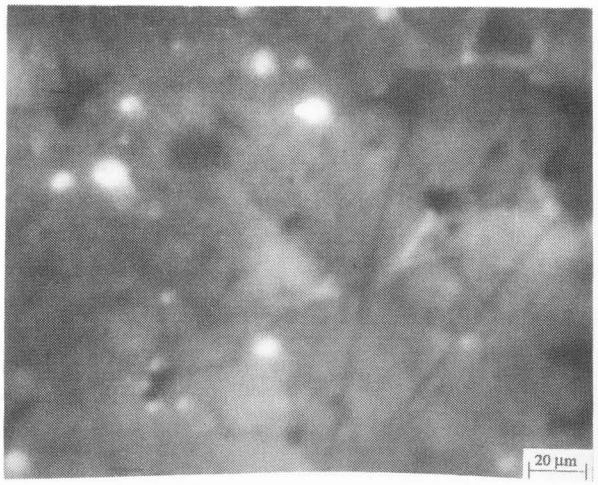

Figure 9. CL micrograph from sample R2 annealed in a strongly reducing atmosphere at 293K.

---

boundary, are distinguishable.

In Figures 8 and 9, the room-temperature CL micrographs taken in the visible spectral range from samples R1 and R2 annealed in reducing atmosphere are shown. Obviously, after annealing in a weakly reducing atmosphere the typical CL contrast is conserved. Annealing in a strongly reducing atmosphere, however, causes the CL contrast to vanish. No change in the spectral composition of the CL signals from grain and grain-boundary zones could be observed in both cases.

The temperature-dependent CL experiments on sample R1 yielded the same results as on the as-received samples. In Figure 10, the logarithm of the integral CL signal from sample R2 is plotted over the reciprocal temperature (1/T). Here, in the strongly reduced specimen, the temperature dependence of the CL intensities from grains and grain boundaries is identical.

Discussion

The results of the spectrally resolved CL observations demonstrate that the predominant CL signal from PTC $BaTiO_3$ ceramics is due to a unique radiative recombination process present both inside the grains and in the grain-boundary region and bearing a maximum at about 2.4 eV. The nature of the dominating radiative recombination mechanism is not yet known. Nevertheless, from extended CL studies on $BaTiO_3$ ceramics with varying dopants, additives and substitutes, that all left the main CL spectrum unaffected (Hübner, 1994), we can exclude that intrinsic and extrinsic acceptor or donor states play a role as radiative recombination centers. Furthermore, the spectral composition of the CL signals from grain and grain boundaries was essentially the same. Thus, a radiative recombination including exciton or polaron states appears to be the most probable mechanism.

To gain more insight into the basic recombination processes, CL studies on $BaTiO_3$ single crystals at low temperatures down to 4.2K are in progress.

If the CL grain-boundary contrast cannot be attributed to differences in the radiative recombination channels in the grain and in the grain-boundary region, than the observed CL behavior should originate in non-radiative recombination processes.

Assuming that in a certain temperature interval, only one dominating non-radiative recombination process is present and the probability for radiative recombination is constant, the temperature dependence of the integral CL signal, I_{CL}, is given (Bimberg *et al.*, 1971) by:

$$(I_{CL} / I_{CL_0}) = [1 / (1 + Ce^{-E_A/kT})] \qquad (1)$$

Here I_{CL_0} denotes an arbitrary chosen reference CL intensity, k is the Boltzmann constant, and C and C^* refer to the total number of non-radiative centers. E_A can be interpreted as an activation threshold for the dominating non-radiative recombination process within any temperature interval, where the slope is constant.

The denominator describes the amount of activated non-radiative recombination centers. If it is considerably larger than 1, then the logarithm of the normalized CL intensity becomes a linear function of 1/T.

$$(I_{CL} / I_{CL_0}) = Ce^{E_A/kT} \qquad (2)$$

and

$$\ln (I_{CL} / I_{CL_0}) = [C^* + \{(E_A/k)\ (1/T)\}] \qquad (3)$$

where $C^* = \ln C$.

In Figure 7, it is shown that in non-reduced samples, the activation energies for the non-radiative recombination processes in the temperature interval from 60K to 185K are different for grain and grain-boundary zones. In the grain interior, the activation energy of the dominating non-radiative recombination process amounts to 30 meV $\pm$ 2 meV, whereas at grain boundaries a value of 36 meV $\pm$ 2 meV is found. Thus, upon cooling, the non-radiative recombination process drops out earlier at grain boundaries than in the grains and the boundaries become brighter than the grains. At approximately 60K, a point is reached, where this non-radiative recombination process has no more influence upon the CL intensity. Below this temperature, the slope of the grain CL intensity is larger and the CL intensities from grains and grain boundaries approximate to each other again.

Figure 10 demonstrates that after annealing in strongly reducing atmosphere (sample R2), inside grains, the same value for E_A is found as for non-reduced samples at grain boundaries. Obviously, during annealing, the characteristic non-radiative recombination centers, initially present in the grain-boundary zones of as-received samples, have spread over the grain interior. Under the present annealing conditions, only oxygen vacancies are volatile, whereas the concentration and distribution of all other impurities or intrinsic defects should not be effected appreciably. Therefore, we conclude that oxygen vacancies, alone or in complexes, are the centers of non-radiative recombination in question.

To prove this quantitatively, we calculated the oxygen vacancy concentration for the as-received and for the annealed $BaTiO_3$ ceramic samples. The oxygen vacancy concentration is sketched in Figure 11 as a function of the acceptor concentration with p_O as parameter. Generally, the oxygen vacancy concentration in thermodynamic equilibrium is a function of temperature, oxygen partial pressure and free electron concentration, for oxygen vacancies act as donors in $BaTiO_3$. For neutrality reasons, the electron density (n) is related to the acceptor concentration. In the grain interior, n is determined by the donor density [D], being 3.2 x 10^{19} cm^{-3} in the case of a 0.2 mol% La doping. According to usual PTC models, the density of acceptor states raises steeply in the grain boundary region and overcompensates the n conductivity. In Figure 11, the vertical dotted line indicates the transition from n to p regions and is suggested to mark the beginning of the grain-boundary zone. This representation is independent of the actual acceptor distribution profile at the grain boundary that would be necessary to redraw the horizontal axis in spatial coordinates.

For the as-received samples, the oxygen vacancy concentration in the grains is very low. By virtue of the neutrality condition at grain boundaries, the oxygen vacancy concentration is enhanced due to the localized acceptor states. In the CL images of these samples, a pronounced contrast is observed with dark grain boundaries at room temperature.

After annealing in strongly reducing atmosphere, the oxygen vacancy concentration is equally high within grains and at grain boundaries. The CL contrast vanishes.

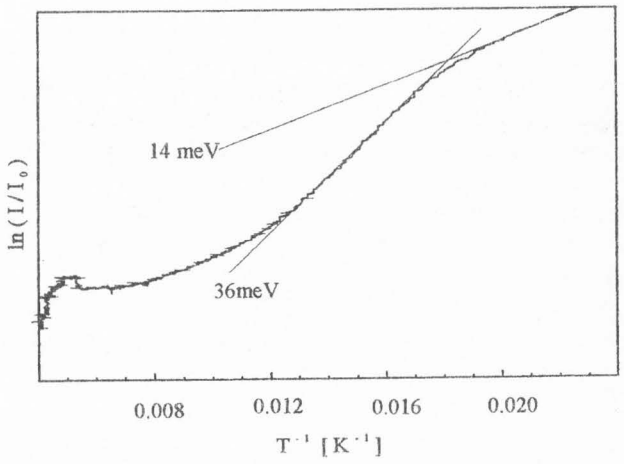

Figure 10. Logarithm of the normalized integral CL intensity versus 1/T taken in the visible spectral range from sample R2.

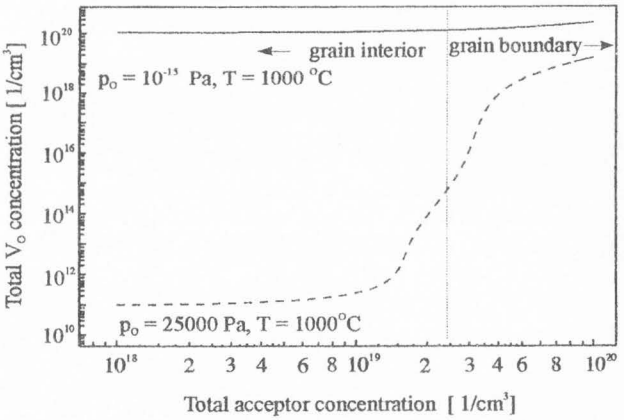

Figure 11. Oxygen vacancy concentration as a function of acceptor concentration. The full line represents the V_O distribution in the strongly reduced sample R2, the dashed line refers to the as-received sample..

Summary

The CL grain-boundary contrast in $BaTiO_3$ PTC ceramics is an intrinsic effect originating from oxygen vacancies localized at grain boundaries. Oxygen vacancies act as non-radiative recombination centers with a typical activation energy of 36 meV. Contrary to earlier statements in the literature, radiative recombination processes are not responsible for the grain boundary contrast. In particular, it could not be confirmed that Ba vacancies give rise to CL transitions in the near IR. Thus, from the CL point of view, the Ba vacancy model for the PTC effect can neither be verified nor rejected at present.

Further investigations into the quantitative details of the recombination processes taking place in semiconducting ceramics are in progress. The results gained so far raise our hopes that temperature-dependent CL spectroscopy and microscopy become an unique and powerful tool for the characterization of defects that escape identification by other methods. A prerequisite for a reliable interpretation of the CL results from ceramic material, however, is a careful high-resolution microanalysis to avoid impurity effects (Marx *et al.*, 1993).

Acknowledgement

The authors thank P. Abicht, T. Langhammer and their coworkers for preparing and characterizing the ceramic samples. We acknowledge the financial support of the Ministerium für Wissenschaft und Forschung des Landes Sachsen Anhalt, Germany, grant numbers 217 A0441 and 034 A03 11 82.

References

Abicht H-P, Langhammer HT, Felgner KH (1991) The influence of silicon on microstructure and electrical properties of La-doped $BaTiO_3$ ceramics. J Mater. Sci. **26**, 2337-2342.

Bimberg D, Sondergeld M, Grobe E (1971). Thermal dissociation of excitons bound to neutral acceptors in high-purity GaAs. Phys. Rev. **B4**, 3451-3455.

Daniels J, Wernicke R (1976). New aspects of an improved PTC model. Part V. Philips Res. Repts. **31**, 544-559.

Hübner T (1994). Katodolumineszenz-Spektroskopie und -Mikroskopie an Bariumtitanatkeramiken. VDI Verlag, Dusseldorf, Germany. pp. 39-87.

Hübner T, Marx U, Hedrich T (1993). IR cathodoluminescence investigations on La-doped barium titanate ceramics. phys. stat. sol. (a) **136**, K61-.

Koschek G, Kubalek E (1983). Micron-scaled, spectral-resolved cathodoluminescence of grains in barium titanate ceramics. phys. stat. sol. (a) **79**, 131-139.

Koschek G, Kubalek E (1985). Grain-boundary characteristics and their influence on the electrical resistance of barium titanate ceramics. J. Am. Ceram. Soc. **68**, 582-586.

Marx U, Hübner T, Schreiber J, Abicht P, Hedrich T, Syrowatka F (1993). Temperature-dependent cathodoluminescence spectroscopy and microscopy and analytical electron microscopy of $BaTiO_3$-based PTC ceramics. In: Third Euro-Ceramics, Vol. 2, Properties of Ceramics. Duran P, Fernandez JF (eds.). pp. 29-34.